

Preprints are preliminary reports that have not undergone peer review. They should not be considered conclusive, used to inform clinical practice, or referenced by the media as validated information.

Magnoflorine alleviates colitis-induced anxiety-like behaviors through regulating gut microbiota and microglia mediated neuroinflammation

Lei Wang wanglei2021@tmu.edu.cn

Tianjin Medical University, Tianjin Institute of Digestive Diseases

Mengfan Li mengfannn@tmu.edu.cn

Tianjin Medical University, Tianjin Institute of Digestive Diseases

Yue Dong dongyue@tmu.edu.cn

Tianjin Medical University, Tianjin Institute of Digestive Diseases

Jingyi Wang *Wangjingyi1105@tmu.edu.cn*

Tianjin Medical University, Tianjin Institute of Digestive Diseases

Siqi Qin qinsiqi@tmu.edu.cn

Tianjin Medical University, Tianjin Institute of Digestive Diseases

Liying Li

liliying868798@163.com

the Affiliated Hospital of Chengde Medical College

Bingqing Li libq68@sohu.com

the Affiliated Hospital of Chengde Medical College

Bangmao Wang *mwang02@tmu.edu.cn*

Tianjin Medical University, Tianjin Institute of Digestive Diseases

Hailong Cao

caohailong@tmu.edu.cn

Tianjin Medical University, Tianjin Institute of Digestive Diseases

Research Article

Keywords: Inflammatory Bowel Disease, Anxiety, Gut-brain axis, Microbiota, Microglia

DOI: https://doi.org/

License:

This work is licensed under a Creative Commons Attribution 4.0 International License.

Read Full License

Additional Declarations: No competing interests reported.

Magnoflorine alleviates colitis-induced anxiety-like
 behaviors through regulating gut microbiota and
 microglia mediated neuroinflammation
 Lei Wang^{1,2,#}, Mengfan Li^{1#}, Yue Dong¹, Jingyi Wang¹, Siqi Qin¹,

5 Liying Li², Bingqing Li², Bangmao Wang¹, Hailong Cao^{1,*}

6 1 Department of Gastroenterology and Hepatology, General Hospital, Tianjin Medical University,

7 National Key Clinical Specialty, Tianjin Institute of Digestive Diseases, Tianjin Key Laboratory of

8 Digestive Diseases, Tianjin 300052, China.

9 ² Heibei Key Laboratory of Panvascular Diseases; Department of Gastroenterology and Hepatology,

10 the Affiliated Hospital of Chengde Medical College, Hebei, China

11 [#] These authors have contributed equally to this work.

12 * Correspondence: Hailong Cao, Department of Gastroenterology and Hepatology, General Hospital,

- Tianjin Medical University, 154 Anshan Road, Heping District, Tianjin 300052, China.
 <u>caohailong@tmu.edu.cn</u>. Telephone: +86-022-60362608, Fax: +86-022-27813550
- 15 Abstract

Background: Inflammatory bowel disease (IBD) and anxiety are often comorbid, and are interconnected through the microbiota-gut-brain axis. The therapeutic medications for anxiety are often constrained by adverse effects that limit their long-term use. The pursuit of natural, safe drug for anxiety is important, with the precise mechanisms elucidating the interplay between drugs and the gut-brain axis in modulating mood remaining elusive.

Results: We revealed a significant association between active ulcerative colitis(UC) patients and anxiety. Mendelian randomisation analysis suggested that UC has a causal relationship on anxiety, but not on depression. Next we identified *Ziziphus jujuba*, a natural plant, as a dual

therapeutic agent for both UC and anxiety through Batman database. 26 27 Magnoflorine, as the predominant compound found in Ziziphus jujuba, exhibits promising therapeutic properties for the treatment of UC and 28 29 anxiety disorders. Our experiments found that magnoflorine not only 30 alleviated colitis, but also reduced colitis-induced anxiety behaviors through 31 gut microbiota. Mechanistically, magnoflorine could increase the abundance of Odoribacteraceae and Ruminococcus, regulate bile acid metabolism, 32 especially hyodeoxycholic acid (HDCA) in colitis mice. HDCA supplement 33 could alleviate both colitis and colitis-induced anxiety. Meanwhile HDCA 34 35 could inhibit the binding site of lipopolysaccharide to the TLR4/MD2 complex, thereby inhibiting microglia activation and alleviating neuroinflammation. 36

37 Conclusion: Our study unveils that magnoflorine alleviates colitis-induced
38 anxiety-like behaviors through regulating gut microbiota and microglia
39 mediated neuroinflammation, which has the potential therapeutic for IBD
40 comorbid with anxiety disorders.

41 Keyword : Inflammatory Bowel Disease; Anxiety; Gut-brain axis; Microbiota;
42 Microglia

43

44 Background

Inflammatory bowel disease (IBD) is a prevalent condition in northern
Europe and North America, with a rapid increase reported in Asia¹. It is
characterized by chronic and incurable inflammation of the gastrointestinal

48 tract. Gut microbial dysbiosis has been consistently associated with intestinal 49 inflammatory diseases, including IBD. Evidence indicates that reduced diversity and richness of gut microbiota correlate with an elevated risk of 50 colitis². The microbiota plays a crucial role in the development of IBD³. 51 Metabolomic and metagenomic profiling have revealed distinct differences in 52 53 microbial and metabolite compositions between IBD patients and healthy 54 individuals⁴. Alterations in the microbiota contribute to IBD through multiple mechanisms. One key mechanism is the production of metabolites by the gut 55 56 microbiota. Specific classes of metabolites, such as bile acids, short-chain 57 fatty acids (SCFAs), and tryptophan metabolites, have been implicated in the pathogenesis of IBD. These metabolites can affect the host through various 58 59 mechanisms, including modulation of immune responses and inflammation⁵.

60 IBD has a high prevalence of comorbid anxiety and depression. Multiple studies have shown that the prevalence of anxiety is increased in patients 61 with IBD compared to the general population. The prevalence for symptoms 62 63 of anxiety in patients with IBD estimates range from 5% to $20.7\%^6$. The anxiety and depression have been associated with a more aggressive 64 65 presentation of IBD⁷. They can also affect disease activity and increase the risk of hospital readmissions in individuals with IBD. Anxiety and IBD are 66 interconnected, with each influencing the other through gut-brain axis⁸. The 67 gut-brain axis is a bidirectional communication system between the gut and 68 69 the brain. It involves complex interactions between the central nervous

70 system (CNS), the enteric nervous system (ENS), the gut microbiota, and the immune system⁹. Changes in the gut microbiota, gut inflammation, and gut 71 72 permeability can affect brain function and contribute to the development of 73 psychiatric symptoms⁶. Individuals with IBD were 34% more likely to initiate 74 antidepressants in the year following IBD diagnosis compared to controls 75 without IBD⁹. The potential benefits of antidepressants in IBD are as follows: 76 treating anxiety and depression; reducing pain and improving sleep¹⁰. Antidepressants can have various side effects, such as gastrointestinal 77 effects, sexual dysfunction, weight changes, dizziness and drowsiness, 78 79 changes in blood pressure and heart rate. The prevalence of antidepressant medication use among patients with IBD has been steadily increasing in 80 recent years. However, a significant proportion of these patients, 81 approximately two-thirds, do not adhere to the full course of treatment⁹. 82 Finding a medication that treats both IBD and anxiety with few side effects is 83 critical. 84

85 Magnoflorine is the main ingredient in *Ziziphus jujuba*, which is heavily used in Chinese medicine to treat insomnia and other neurological disorders. 86 Magnoflorine has a wide range of pharmacological effects, including 87 anti-diabetic activity; anti-inflammatory activity; cardiovascular effects; 88 neuropsychopharmacological activity: anti-anxiety; 89 antifungal activity; 90 immunomodulatory activity and antioxidant activity. Based on the available 91 studies, magnoflorine has shown no cytotoxicity to most cells and has been

92 considered relatively safe¹¹. Hence magnoflorine has a potential function to
93 treat IBD and anxiety with less side effects.

In this investigation, we scrutinized the impact of magnoflorine on gut 94 95 microbiota, and substantiated the amelioration of colitis and anxiety-related behaviors by magnoflorine through three rescue experiments (Antibiotic 96 97 Intervention Experiment, fecal microbiota transplantation and sterile fecal filtrate transplantation), and then elucidated the mode of action of 98 99 magnoflorine on colitis and colitis-induced anxiety. Relying on intestinal 100 microbiota and their metabolites, we subsequently probed the pivotal 101 intestinal bacterial metabolite hyodeoxycholic acid (HDCA), and 102 comprehensively probed the mechanism of action of HDCA on neuroinflammation via modulation of the TLR4/Myd88 pathway. 103

104

105 Methods

106 **Clinical investigation**

Patients diagnosed with UC from four hospitals participated in the completion of clinical questionnaires assessing anxiety, depression, sleep quality, and overall quality of life. Questionnaires utilized for this evaluation included Generalized Anxiety Disorder 7-item Scale (GAD-7), Patient Health Questionnaire- 9 (PHQ-9), Pittsburgh Sleep Quality Index (PSQI), and Inflammatory Bowel Disease Quality-of-Life Questionnaire (IBD-Q)

113 Inclusion criteria for this study encompassed individuals diagnosed with

UC and age \geq 18. Exclusion criteria involved patients who declined 114 participation in the clinical survey, individuals lacking comprehension of the 115 questionnaire content, those with documented mental disorders, comorbid 116 117 malignant tumors, neurological disorders, chronic disorders affecting systems beyond the gastrointestinal tract, such as heart disease and renal 118 119 conditions, as well as those incapable of self-care. The clinical investigation was approved by the ethics committee of the Tianjin Medical University, 120 121 Tianjin, China (Approval NO. IRB2024-YX-152-01)

122

123 Mendelian randomisation

We used two-sample MR to assess causality mediating between UC, 124 anxiety and depression. All data were publicly available genome-wide 125 association studies (GWAS) summary statistics. GWAS searches of summary 126 statistics were performed to extract polymorphic genetic instrumental 127 variables(IVs) for single nucleotide polymorphisms (SNPs) associated with 128 129 UC, anxiety or depression. The genetic data for UC and depression were 130 obtained from a recently published paper¹². And genetic data for anxiety were obtained from PGC dataset. The IVs were chosen based on the 131 following criteria: (1) SNPs associated with each genus at the genome-wide 132 motif significance threshold ($P < 1.0 \times 10^{-7}$ for UC, $P < 1.0 \times 10^{-7}$ for anxiety, 133 $P < 1.0 \times 10^{-8}$ for depression) were identified as potential IVs; (2) The 134clumping parameters were set to $r^2 < 0.001$, and kb = 10,000 kb in order to 135

ensure independence among the selected SNPs; (3) Positive stranded alleles 136 137 were used to infer positive stranded alleles using allele frequency information when palindromic SNPs were present. Next, the strength of the 138 139 IVs was examined using F-values (F=[beta/Se]2), weak IVs with F<10 were removed. We mainly applied inverse variance weighted (IVW) as the main 140 analysis to combine the SNP-speciffc estimates calculated using Wald 141 ratiosto, for detecting the effect of UC on anxiety and depression or anxiety 142 143 and depression on UC. We first harmonized the exposure and outcome data to comparison of effector alleles in the positive strand, if specific or can be 144 145 inferred based on allele frequencies. Echoes of the gene variants were discarded for further MR analysis. Next, Mendelian randomization analysis, 146 heterogeneity test, multiple validity test, and graphing were performed using 147 148 TwosampleMR package in R(version: 4.3.1). In addition, we applied Leave-one-out analysis to assess the impact of each SNP on the estimation. 149

150

151 Animal experiments

Specific pathogen free (SPF)-grade female C57BL/6J mice, aged 6-8 weeks, were obtained from Fukang (Beijing, China) and housed in the SPF-grade animal facility at the Affiliated Hospital of Chengde Medical College. The mice were housed in groups of 4-5 per cage and provided with a standard pellet diet and ad libitum access to water. The animal facility maintained a controlled environment with a 12-hour light/dark cycle and a temperature of

158 25 ± 2 °C. Following a 7-day acclimatization period, a colitis model was
159 induced by administering 3% DSS (40 KDa) in the drinking water for a
160 duration of 7 days. All animal experiments were approved by the ethics
161 committee of the Tianjin Medical University, Tianjin, China (Approval No.
162 IRB2022-DWFL-074)

163 Magnoflorine intervention

Thirty-two C57BL/6J mice were weighed after a one-week acclimatization 164 period following their purchase. The experiment commenced when their 165 body weight reached approximately 20 g. The mice were divided into four 166 167 experimental groups, each receiving different treatments. The groups and treatments were as follows: 1. Control group: mice were provided with free 168 access to water and received PBS solution by gavage.2. Mag group: mice 169 170 were provided with free access to water and received PBS solution containing magnoflorine (10 mg/Kg/d) by gavage for 10 days. 3. DSS group: 171 mice were provided with free access to water for the first three days, 172 173 followed by ad libitum access to 3% DSS for the remaining seven days. They received PBS solution by gavage. 4. Mag + DSS group: mice were provided 174 with free access to water for the first three days, followed by ad libitum 175 access to 3% DSS for the remaining seven days. They received PBS solution 176 containing magnoflorine by gavage(10 mg/Kg/d) for 10 days. The optimal 177 administration concentration of magnoflorine was determined through our 178 179 pre-experimental validation process.

Antibiotic Intervention Experiment: Eighteen 6-8-week-old C57BL/6 mice were divided into three groups: ABx-C, ABx-D, and ABx-MD. The experimental procedures for each group were the same as the Control, DSS, and Mag + DSS groups, respectively. However, before the colitis model was induced, the mice in all three groups were given an antibiotic cocktail (penicillin 200 mg/L, neomycin 200 mg/L, metronidazole 200 mg/L, and vancomycin 100 mg/L) ad libitum for 2 weeks.

187 During the course of the experiment, the body weight of the mice was recorded on a daily basis. The disease activity index (DAI) score was utilized 188 189 to evaluate the severity of colitis based on weight loss, stool condition, and 190 the presence of blood in the stool¹³. On the fifth day of the experiment, fecal samples were collected from each group of mice and stored at -80°C for 191 192 further analysis. On the eighth day, under chloral hydrate anesthesia, Brain tissues were obtained and the hippocampal region were isolated. Some of the 193 brain tissue samples were partially frozen at -80°C, while others were fixed in 194 195 10% formalin for subsequent investigations. The entire colon was collected, 196 and the length was measured. A portion of the colon tissue was frozen at -80°C, while the other portion was fixed in 10% formalin for further studies. 197

198 FMT and SFF

199 In the present study, we conducted experiments in which we 200 simultaneously concurrently provided nourishment to 10 mice, serving as 201 fecal donors for subsequent fecal microbiota transplantation (FMT) and

202 sterile fecal filtrate (SFF). The feeding conditions were consistent with those 203 mentioned earlier. Additionally, we administered PBS/Mag to two separate groups of mice via oral gavage, with each group consisting of 5 mice. This 204 205 administration was carried out for a duration of 8 days, followed by a 206 cessation period of 3 days. The purpose of this cessation was to collect fecal 207 samples for subsequent FMT and SFF procedures. Then we collected the stool and dissolved that in sterile PBS at a ratio of 200 mg feces to 2 ml PBS 208 209 and mixed thoroughly. The suspension was filtered through a sterile 700 210 mesh filter and subsequently centrifuged at 600 g for 5 minutes. This process 211 allowed for the collection of the supernatant, which was used for FMT. The supernatant was further filtered through a sterile 0.22 um filtration 212 membrane to ensure sterility before being used for SFF¹⁴. 213

FMT: Twelve 6-8-week-old C57BL/6 mice were divided into two groups: FMT-Control and FMT-Mag. After 2 weeks of antibiotic cocktail intervention, the mice in both groups received fecal bacteria via gavage for 3 days at a volume of 200 ul/day. Following the fecal transplantation, the mice in both groups were given ad libitum access to 3% DSS for 5 days.

219 SFF: Twelve 6-8-week-old C57BL/6 mice were divided into two groups: 220 SFF-Control and SFF-Mag. After 2 weeks of antibiotic cocktail intervention, 221 the mice in both groups received a colony metabolite transplantation via 222 gavage for 10 days at a volume of 200 ul/day. In the last 5 days, the mice in 223 both groups were given ad libitum access to 3% DSS for 5 days.

224 HDCA intervention

Twenty 6-8-week-old C57BL/6 mice were divided into four groups: 1. 225 Control group: mice were provided with free access to water and received 226 227 0.5% carboxymethylcellulose sodium(CMC) solution by gavage. 2. HDCA group: mice were provided with free access to water and received 0.5%CMC 228 229 solution containing HDCA (500 mg/Kg/d) by gavage for 10 days. 3. DSS group: mice were provided with free access to water for the first three days, 230 231 followed by ad libitum access to 3% DSS for the remaining seven days. They received 0.5%CMC solution by gavage. 4. HDCA + DSS group: mice were 232 233 provided with free access to water for the first three days, followed by ad libitum access to 3% DSS for the remaining seven days. They received 234 0.5%CMC solution containing HDCA by gavage(500 mg/Kg/d) for 10 days¹⁵. 235

236

237 Behavioral Experiments

The mice were given a 30-minute acclimatization period upon entering the 238 239 laboratory room from the rearing room before the behavioral experiments began. During this acclimatization period, the mice were allowed to adjust to 240 their new environment. After the acclimatization period, the behavioral 241 experiments were initiated. The activities of each mouse were recorded for a 242 total of 5 minutes. However, for the analysis, only the activities of the mice 243 during the last 4 minutes of the recording were analyzed using ImageJ 244 245 software. The software was used to analyze and quantify the specific behaviors or activities exhibited by the mice during this time period.

1. Open Field Test (OFT): The Open Field Test is commonly used to assess
the anxiety level and locomotor/exploratory ability of mice. In this test, mice
are placed in an open arena (50 x 50 x 50 cm) and their behavior is recorded.
Parameters such as total movement distance, central area movement
distance, and central area exploration time are measured and analyzed to
evaluate the mice's locomotor and exploratory abilities.

2. Elevated Plus Maze Test (EPT): The Elevated Plus Maze Test is another
commonly used test to assess anxiety levels and exploratory behavior in mice.
The maze consists of two open arms and two closed arms, elevated above the
ground. Mice are placed on the maze and their behavior is recorded.
Parameters such as exploration time in the open arm, stay time in the closed
arm, and the number of times entering the open arm are measured to assess
the mice's exploratory abilities and anxiety levels.

3. Tail Suspension Test (TST): The Tail Suspension Test is used to assess
depression-related behaviors in mice. In this test, mice are suspended by
their tails for a specific period of time, and their immobility time is recorded.
Increased immobility time is considered an indicator of depressive-like
behavior.

4. The Forced Swimming Test (FST) was employed to evaluate
depression-related behaviors in mice. A transparent vessel with dimensions
of 30 cm in height and 20 cm in diameter was utilized for this experiment.

The vessel was filled with tap water, and the temperature was maintained at 269 23-25°C. The liquid level in the vessel was standardized for each experiment. 270 The mice were gently grasped by their tails and placed vertically into the 271 water-filled vessel. The duration of immobility, defined as the absence of any 272 active movement, was recorded during the test.

These behavioral tests are commonly used in preclinical research to assess the effects of various interventions or conditions on the behavior of mice, including anxiety and depression-related behaviors.

276

277 Histology analysis and PAS staining

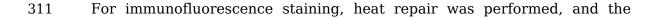
Formaldehyde-fixed colon tissues were processed to create paraffin 278 sections with a thickness of 5 micrometers. This was done by treating the 279 tissues with a series of alcohol gradients, followed by xylene and paraffin 280 embedding. Hematoxylin-eosin (H&E) staining was then applied to the 281 sections. The stained sections were analyzed using ImageJ software to 282 283 evaluate various aspects of the tissue pathology, including inflammatory infiltration, crypt structural alterations, and ulceration. The software was 284 used to analyze the images and assign scores to quantify the severity of these 285 pathological features¹⁶. In addition to hematoxylin-eosin staining, periodic 286 acid Schiff (PAS) staining was conducted on paraffin-embedded tissue 287 sections. The procedure involved dewaxing in xylene, rehydration in ethanol, 288 289 and rinsing in distilled water. Sections were oxidized with periodic acid for

290 15 minutes, then stained with Schiff reagent for 10 minutes and rinsed again 291 for 5 minutes. Counterstaining with hematoxylin was performed for 1 minute, 292 followed by washing, dehydration, and sealing with neutral resin for 293 microscopic examination. The number of positive cells in each crypt was 294 subsequently counted.

295

296 Immunohistochemistry and immunofluorescence staining

297 Colorectal and brain tissues were processed into paraffin sections with a thickness of 5 micrometers. The sections underwent a series of steps 298 299 including xylene treatment, gradient alcohol dehydration, thermal repair 300 using citrate buffer, and antibody incubation. For the colon tissue, MUC2 antibody (1:1000, PROTEINTECHGROUP, USA) was used, while for the 301 302 hippocampal tissue, IBA1 antibody (1:300, ABclonal, Wuhan, China) was employed. The incubation with primary antibodies was carried out overnight 303 at 4°C, followed by washing with PBS three times for 3 minutes each. 304 305 Subsequently, the sections were subjected to secondary antibody incubation 306 for 20 minutes, followed by another round of PBS washing. Diaminobenzidine hydrochlo-ride (DAB) stain was performed for 1 minute, and the sections 307 308 were observed after sealing. The number of MUC2-positive cells in each colonic crypt was counted, and the morphology of microglia was evaluated 309 310 using ImageJ software.



312 colon and hippocampal tissue sections were blocked with 5% goat serum for 313 20 minutes. Anti-PV1(1:200, ABclonal, Wuhan, China), anti-ZO-1(1:200, 314 ABclonal, Wuhan, China) were incubated with the sections for 48 hours at 315 4°C. After washing with PBST (PBS with Tween-20) three times for 5 minutes each, the sections were incubated with fluorescent secondary antibodies for 316 317 1 hour. Following another round of PBST washing, the nuclei were stained with 4',6-Diamidino-2'-phenylindole (DAPI). The sections were washed again 318 with PBST and sealed with an antifluorescent mounting medium for 319 320 fluorescence microscopy. The relative fluorescence intensity was evaluated 321 using ImageJ software.

322

323 Cell culture and drug treatment

The BV2 microglia cell line was purchased from the Chinese Type Culture 324 microglia BV2 325 Conservation Centre. cells cultured were in Dulbecco's-modified Eagle's medium F12 (DMEM F12) (Gibco; Thermo 326 327 Fisher Scientific, Inc.) supplemented with 10% fetal bovine serum (FBS) (Gibco; Thermo Fisher Scientific, Inc.) with 1% penicillin/streptomycin at 328 37°C in an incubation environment of 5% CO₂. BV2 microglia cells were 329 implanted into 6-well plates and treated with HDCA (25uM, 50uM, 100uM) 330 for 1 h, followed by Lipopolysaccharide (LPS 100ng/ml) for 24 hr. Cells were 331 332 subsequently collected to extract the total RNA and protein for RT-PCR and 333 WB.

334

335 Real-time polymerase chain reaction

Total RNA was extracted from intestinal and brain tissues using the 336 337 RNeasy mini kit (Qiagen, Carlsbad, CA, USA), with RNase-free water used for elution. The concentration and purity of the obtained RNA were assessed 338 339 using a nano drop spectrophotometer (Thermo Fisher Scientific, USA). For cDNA synthesis, 1000 ng of total RNA per sample was utilized and reverse 340 341 transcribed using the TIANScript RT kit according to the manufacturer's instructions (TIANGEN, Inc. Beijing, China). Real-time PCR analysis was 342 343 performed using the StepOnePlus Real-time PCR system (Applied Biosystems, Thermo Fisher Scientific, Waltham, MA). The primer sequences for target 344 genes are provided in Additional file 2: Table S1. 345

346

347 Western blotting

Tissue samples were lysed in RIPA buffer containing protease and 348 phosphatase inhibitors. The proteins 349 were then separated by SDS-polyacrylamide gel electrophoresis and transferred onto a polyvinyl 350 dene fluoride (PVDF) membrane. Then the membrane was blocked in 5 % 351 BSA at room temperature for 20 min. Subsequently, the primary anti-CLDN3 352 (1:1000, Cell Signaling Technology, Danvers, MA, USA), anti-ZO-1(1:1000, 353 ABclonal, Wuhan, China), anti-TLR4(1:1000, Cell Signaling Technology, 354 355 Danvers, MA, USA), anti-Myd88(1:1000, Cell Signaling Technology, Danvers,

MA, USA), anti-IL-6(1:1000, Cell Signaling Technology, Danvers, MA, USA), 356 357 anti-β-actin (1:5000, Cell Signaling Technology, Danvers, MA, USA) and anti-GAPDH(1:1000, ABclonal, Wuhan, 358 China) were suppled. The 359 chemiluminescent signal was detected using ECL following incubation with appropriate secondary antibodies. Band intensity was analyzed using ImageJ. 360

361

362 Molecular docking analysis

The amino acid sequence and protein domain were retrieved from PDB database (https://www.rcsb.org/). The structure of HDCA was retrieved from PubChem database. The TLR4/MD2/LPS complex was retrieved from PDB database, which was then visualized in PyMOL software (Schrodinger). The ligand-binding domain of TLR4/MD2 complex to HDCA was as the same as to LPS. The ligand was docked to TLR4/MD2 complex in Autodock software, which was then visualized in PyMOL software.

370

371 Gut microbiota analysis

16S rRNA gene sequencing was performed at the Sangon BioTech Institute
(Shanghai, China) to analyze the microbial composition. Genomic DNA
extraction from the total community was carried out using the E.Z.N.A[™]
MagBind Soil DNA Kit (Omega, M5635-02, USA). The V3-V4 region of the
16S rRNA gene was amplified using the 2x Hieff® Robust PCR Master Mix
(Yeasen, 10105ES03, China) with specific PCR primers: forward primer

378 (CCTACGGGNGGCWGCAG) and primer reverse 379 (GACTACHVGGGTATCTAATCC). The PCR products were then subjected to sequencing using the Illumina MiSeg system (Illumina MiSeg, USA). The 380 381 resulting sequence tags were clustered into operational taxonomic units (OTUs) with a \geq 97% similarity threshold using Usearch software (version 382 383 11.0.667). Principal coordinates analysis (PCoA) and analysis of similarities (ANOSIM) with a 999 permutations were employed to assess whether 384 385 inter-group differences were significantly greater than intra-group differences. Differences between groups were compared using Statistical 386 387 Analysis of Metagenomic Profiles (STAMP) (version 2.1.3) and Linear discriminant analysis (LDA) effect size (LEfSe) (version 1.1.0). Correlation 388 coefficients and p-values between microbial communities/OTUs and mouse 389 390 characteristics were calculated using the Weighted correlation network analysis (WGCNA) package in R software (version 4.3.1). 391

392

393 **RNA sequencing analysis**

RNA sequencing analysis was performed by Sangon Biotech, Inc. (Shanhai,
China). Total RNA was extracted from colon tissues using the Total RNA
Extractor (Sangon Biotech , Shanhai, China). Quality and quantity of RNA
was analysed by Qubit2.0 RNA kit and Bioanalyzer FR-980A(FURI Science,
Shanhai, China). Samples were submitted to Sangon Biotech for library
preparation, using Hieff NGS[™] MaxUp Dual-mode mRNA Library Prep Kit

and sequencing using DNBSEQ-T7 platform (Illumina). Further analyses
were performed by R software, including alpha diversity, PCoA, differential
expression analysis, GO analysis, KEGG analysis.

403

404 **LC-MS**

405 The main BA profiles in brain were determined by Liquid Chromatograph Mass Spectrometer (LC-MS). The brain sample weighing 30 mg was 406 prepared by adding 100 µL of water and 500 µL of pre-cooled methanol 407 408 solution. Subsequently, 10 µL of 200 ng/mL internal standard was added, 409 followed by vortexing for 60 seconds. The sample was subjected to 410 low-temperature sonication for 30 minutes, repeated twice, and then left at -20°C for 1 hour. Afterward, an additional 10 µL of 200 ng/mL internal 411 412 standard was added, vortexed for 60 seconds, sonicated at low temperature 413 for 30 minutes (twice), and left at -20°C for 1 hour. The resulting mixture was subjected to centrifugation at 14,000 rcf at 4°C for 20 minutes. The 414 415 supernatant was collected and freeze-dried. The BA concentration was 416 quantified using LC-MS.

417

418 Statistical analysis

All data were represented as means±SEM and analyzed using GraphPad
Prism 9.0 program. Data from two groups were compared using
independent-samples t-test, while comparisons among more than two groups

422 utilized one-way ANOVA followed by Tukey's multiple comparison tests. A
423 p-value of less than 0.05 was considered statistically significant.

424

425 **Result**

426 UC combined with anxiety and depression affects patients' quality of 427 life

428 A total of 137 patients with UC were included, including 90 patients with 429 active stage and 47 patients with remission. Age, gender and weight were 430 not associated with disease activity in UC patients (P > 0.05) (Additional file 431 2: Table S2).

We found the proportion of anxiety during the active stage was 432 significantly higher than in remission (P < 0.05), with notable differences in 433 anxiety severity across varying disease activity levels (P < 0.05). Similarly, 434 the proportion of depression in the active stage exceeded that in remission (P435 < 0.05), and differences in depression severity were also significant among 436 different disease activity levels (P < 0.05). Furthermore, the proportion of 437 sleep disturbances was significantly higher in the active stage compared to 438 remission (P < 0.05), although no differences were found across disease 439 440 activity levels (P > 0.05). Additionally, the proportion of individuals experiencing poor quality of life was significantly greater in the active stage 441 (P < 0.05) than in remission (Additional file 2: Table S3, Table S4 and Fig. 442 443 1A).

Moreover, the GAD-7, PHQ-9, and PSQI scores were higher in active UC 444445 than in remission (P < 0.05), and the IBD-Q scores were smaller in active UC (P < 0.05) than in remission (Additional file 2: Table S5). Linear regression 446 447 analyses of GAD-7 and PHQ-9 with PSQI and IBD-Q scores revealed that anxiety ($R^2 = 0.379$, P < 0.0001), depression ($R^2 = 0.475$, P < 0.0001) and 448 quality of life were linearly correlated, while anxiety ($R^2 = 0.072$, P <449 0.0001), depression ($R^2 = 0.145$, P < 0.0001) and sleep disturbances were 450 451 linearly correlated (Fig. 1B). These results suggested that UC combined with anxiety and depression affected the progression of disease and the quality of 452 453 life.

454

455 Bidirectional two-sample Mendelian randomization revealed UC has 456 causal relationship on anxiety

457 Previous investigations have unveiled a proximal interplay among anxiety, depression, and UC through observational methods. However, the precise 458 459 direction of causation remains obscure. Herein, we expounded upon the causal associations between anxiety, depression, and UC employing a 460 bidirectional two-sample Mendelian randomization approach. According to 461 the selection criteria of IVs, the SNPs were used as IVs (Additional file 2: 462 Table S6-S9). Our study disclosed that UC exhibited a notable linkage with 463 anxiety (OR: 1.069, 95% CI: 1.023-1.117, *P* < 0.01), while its correlation with 464465 depression was statistically nonsignificant (OR: 1.047, 95% CI: 0.928-1.183,

466 P = 0.454) in the forward regression. Notably, no inheritable predisposition 467 toward anxiety manifests a relationship with UC upon reverse analysis (OR: 1.005, 95% CI: 0.839-1.206, *P* = 0.949). In contrast, our bidirectional 468 469 Mendelian randomization assessments fail to corroborate a significant 470 association between UC and depression (Fig. 1C). Subsequent scrutiny through tests for heterogeneity (P > 0.05) and horizontal polytropy (P > 0.05) 471 on IVs attests to the absence of heterogeneity or horizontal polytropy. 472 Mendelian randomization exclusion sensitivity analysis revealed that 473 removing any specific SNP did not affect the results (Additional file 1: Fig. 474 475 S1).

476

477 Magnoflorine has potential ability to treat UC and anxiety

478 Utilizing the GeneCards and Batman databases, we employed a targeted approach for pharmaceutical screening to address the therapeutic 479 management of UC and anxiety disorders (Fig. 480 2A). Initially, а 481 comprehensive search operation was conducted in the GeneCards database to identify genes associated with UC and anxiety, setting a stringent 482 threshold (Scores > 5), utilizing the keywords "Ulcerative colitis" and 483 484 "Anxiety". This exploratory phase yielded a remarkable total of 728 genes linked to UC and 190 genes linked to anxiety, with an intriguing convergence 485 of 46 genes overlapped between the two conditions, thereby implicating 486 these specific genetic loci in the co-occurrence of UC and anxiety. 487

488 Subsequent interrogation of the Batman database targeted TCM associated 489 with the identified 46 overlap genes. Intriguingly, our analysis underscored Ziziphus jujuba as the TCM exhibiting the strongest association with these 490 491 genetic targets (P = 7.41e-28). Delving into the pertinent literature 492 pertaining to Ziziphus jujuba, we uncovered documented evidence regarding its potential efficacy in ameliorating symptoms of UC and anxiety^{17,18}. While 493 494the precise mechanistic underpinnings remain unexplored, our investigative 495 foray unveiled Magnoflorine as the principal bioactive constituent of Ziziphus jujuba, renowned for its diverse pharmacological attributes encompassing 496 497 anti-inflammatory and antidepressant properties^{19,20}. Motivated by these intriguing findings, we prioritize Magnoflorine as the focal point of our 498 investigative pursuits to delineate its therapeutic impact on experimental 499 500 colitis and anxiety-related behaviors through meticulously designed animal 501 experimentation protocols.

502

503 Magnoflorine alleviated DSS-induced colitis

To evaluate the effect of magnoflorine on colitis, we induced a mouse model of colitis with 3% DSS orally for 7 days, and observed the phenotype of mice after administration of magnoflorine (10 mg/Kg/d) by gavage. The experimental procedure is shown in Fig. 2B. We determined the optimal concentration of magnoflorine in our previous pre-experiments.. In contrast to DSS, magnoflorine significantly alleviated DSS-induced colitis, and the

510 relevant evidence was that magnoflorine reversed weight loss, decreased 511 DAI scores (Fig. 2C), and alleviated colon length shortening (Fig. 2D). Pathological analyses further indicated that magnoflorine reduced colonic 512 513 inflammatory cell infiltration, decreased crypt destruction, and lowered pathological scores (Fig. 2F). To further investigated the effect of 514 515 magnoflorine on colonic inflammation, we examined the levels of pro-inflammatory factors in colonic tissues. As shown in Fig. 2E, compared 516 517 with the DSS group, the mRNA levels of TNF- α , IL-1 β , and IL-6 were reduced in the Mag+DSS group.Taken together, these results demonstrated that 518 519 magnoflorine can alleviate colitis symptoms and colonic damage in mice with colitis 520

The colonic epithelial barrier plays a pivotal role in the pathogenesis of IBD, 521 and tight junctions are critical components of the colonic epithelial barrier. 522 In our study, we observed reduced expressions in tight junctions including 523 ZO-1 and Claudin 3 in colitis mice through western blotting, while 524 525 magnoflorine treatment effectively reversed this decline (Fig. 3A). Additionally, we employed immunofluorescence staining to investigate the 526 expression of ZO-1. Our data exhibited a decline in ZO-1 expression in colitis 527 mice (Fig. 3B), which was attenuated by magnoflorine treatment. The mucins 528 secreted by goblet cells are crucial for maintaining intestinal barrier 529 integrity and preventing the infiltration of intestinal microbiota. In this study, 530 531 we employed the PAS staining to assess the numbers of goblet cells in

532 colonic tissues. As shown in Fig. 3C, our findings revealed that magnoflorine effectively counteracted the reduction in goblet cell numbers observed in 533 colitis. Furthermore, we employed immunohistochemical staining to examine 534 the expression of MUC2, a key mucin protein, in the colonic tissues of 535 colitis-induced mice. The results demonstrated a significant decrease in 536 537 MUC2 expression, which was mitigated by the administration of magnoflorine. Collectively, these findings suggest that magnoflorine exerts 538 539 its protective effects against DSS-induced colitis by preserving goblet cell function and maintaining the integrity of tight junctions. 540

541

542 Magnoflorine alleviated anxiety-like behaviors in mice with colitis

Patients with colitis often experience comorbid neurological disorders, 543 such as anxiety and depression. In our study, we aimed to assess anxiety and 544 depressive behaviors in mice subjected to colitis induction. To evaluate 545 anxiety-like behaviors, we conducted the OFT and observed a reduction in 546 547 exploration time and distance in the central area among colitis-induced mice. Additionally, in the EPT, colitis mice exhibited decreased exploration time 548 and distance in the open arms, as well as a decrease in the number of entries 549into the open arms. These findings collectively indicated the presence of 550 anxiety-like behaviors in colitis mice. However, treatment with magnoflorine 551 reversed these results (Fig. 4A, Additional file1: Fig. S2), as evidenced by 552 553 increased exploration time and distance in the center area of the OFT, as

well as increased exploration time in open arms, time in close arms, and the
number of entries into the open arms in the EPT. Thus, our results
demonstrated that magnoflorine ameliorated anxiety-like behaviors in colitis
mice.

558 Furthermore, we investigated depressive-like behaviors in mice using the 559 FST and the TST (Additional file1: Fig. S2). Surprisingly, acute colitis 560 induced by DSS did not elicit depressive-like behaviors in the mice. Moreover, 561 magnoflorine did not exert any impact on these behaviors.

562

563 Magnoflorine ameliorated neuroinflammation, reduced microglia 564 activation and maintained blood-brain barrier

Anxious behavior in colitis mice has been reported to be associated with 565 the blood-brain barrier²¹. Thus, we investigated on the blood-brain barrier, 566 specifically focusing on ZO-1 and PV1(Fig. 4B). To demonstrate the impact, 567 we employed immunofluorescence staining and our findings revealed a 568 569 reduction in the expression of ZO-1 and PV1 within the choroid plexus of the lateral ventricle in mice with colitis. Intriguingly, the administration of 570 magnoflorine successfully counteracted this decrease, and these results 571 suggested that magnoflorine could maintain the blood-brain barrier. 572

573 Moreover, we assessed the activation level of microglia in the CA1 region 574 of the hippocampus using immunohistochemical staining to label the 575 expression of IBA1. As shown in Fig. 4C, our findings revealed that microglia

in the CA1 region of the hippocampus of colitis mice exhibited significant
activation, and treatment with magnoflorine reversed this activation, as
evidenced by the reduction in endpoints, and an increase of protrusion
length , indicating its potential to modulate microglial activation.

Given the association between neuroinflammation and anxiety behavior, we 580 sought to investigate the levels of pro-inflammatory factors in the 581 hippocampal region of each experimental group. Our results indicated that 582 colitis mice exhibited elevated expression of mRNA levels of TNF- α , IL-1 β , 583 and IL-6 (Fig. 4D). However, treatment with magnoflorine significantly 584 585 reduced the expression of mRNA levels of pro-inflammatory factors. Collectively, these results suggest that magnoflorine may exert its protective 586 effects against anxiety behavior by modulating neuroinflammation and 587 microglial activation in the hippocampal region. 588

589 Magnoflorine regulated gut microbiota and promoted the enrichment

590 of secondary bile acids-producing bacteria

Next, we further explored the impact of magnoflorine on the gut microbiota composition of each group via 16S rRNA gene sequencing. Magnoflorine increased the Alpha diversity of gut microbiota as shown by shannon index (Additional file1: Fig. S3A). Principal Coordinate Analysis (PCoA) revealed a distinct segregation among all experimental groups (Additional file1: Fig. S3B). Simultaneously, we observed a consistent fecal bacterial composition among all groups of mice at both the phylum and

598 genus levels. But in mice with colitis, the administration of magnoflorine 599 resulted in a reduction of the Firmicutes phylum, an increase in the Verrucomicrobia phylum, and a decreased the Firmicutes/Bacteroidetes ratio 600 601 (Fig. 5A). As shown in Fig. 5B and C, the application of LEfSe analysis 602 revealed an enrichment of specific bacterial taxa within the Mag group at the family level, including Odoribacteraceae, Clostridiales Incertae Sedis XIII, 603 604 Erysipelotichaceae, Streptomycetaceae, Eubadteriaceae, Pdrphyromohadaceae, and Sutterellaceae, additionally, an enrichment of 605 Odoribacter. Longibaculum, 606 Ihubacter, Amedibacillus, Streptomyces, 607 Anaerofustis, Parabacteroides and Parasutterella were observed at the genus level (LDA score > 2.0, P < 0.05). After DSS treatment, *Bifidobacteriaceae*, 608 Oxalobacteraceae and SpirocHaetaceae were enriched at the family level in 609 Mag+DSS group, and Bifidobacterium, Ruminococcus, Butyricicoccus, 610 Lachnospira and Rectinema were enriched at the genus level in Mag+DSS 611 group(LDA score > 2.0, P < 0.05). Bifidobacterium, Ruminococcus, 612 613 Oxalobacteraceae and Butyricicoccus play a role in the regulation of bile acid metabolism²²⁻²⁵. In addition, we utilized the STAMP software to conduct an 614 in-depth analysis of the dissimilarities between the experimental groups. 615 Consistently, our findings revealed an enrichment of Odoribacteraceae in the 616 Mag+DSS group (Additional file1: Fig. S3C), which is known to possess a 617 secondary bile acid metabolism capability²⁶. Subsequently, we employed the 618 619 PICRUSt technique to predict the functional attributes of the groups,

followed by a differential analysis using the STAMP software. Intriguingly,
our results indicated a higher expression of the baiH gene in the Mag+DSS
group compared to the DSS group (Additional file1: Fig. S3D). Notably, this
gene is associated with secondary bile acid metabolism.

To delve deeper into the intricate association between microbial colonies 624 625 and their corresponding traits, we employed the WGCNA approach. This method enabled us to cluster and establish a network of Operational 626 Taxonomic Units (OTUs). Furthermore, we performed power calculations 627 with a value of 7 to enhance the accuracy and reliability of our analyses 628 629 (Additional file1: Fig. S3E). Finally, we successfully constructed sixteen OTU coexpression modules through our analysis. As shown in Fig. 5D, among 630 these modules, the blue module (eigengene value = 0.77, P = 0.001) 631 exhibited the strongest association with EPT(frequency of visits to open 632 arms), while the red module (eigengene value = 0.62, P = 0.02) 633 demonstrated the highest correlation with Mag+DSS. These two modules 634 635 were subsequently chosen for further investigation and analysis. At the family taxonomic level, the Red module encompasses a total of 7 microbial 636 colonies, while the Blue module consists of 47 colonies. Notably, 4 colonies 637 are overlapped between these two modules (Additional file1: Fig. S3F). 638 These overlapping colonies are identified as unclassified Bacteroidales, 639 640 Lachnospiraceae, Ruminococcaceae, and Muribaculaceae.

642 Magnoflorine alleviated colitis and anxiety-like behavior depending 643 on microbiota

In light of the previous findings demonstrating the potential of 644 magnoflorine to enhance the intestinal microbiota in mice, we sought to 645 further investigate the role of the intestinal microbiota in this context. To 646 647 achieve this, we employed a three-step experimental approach. Firstly, we administered an ABx to the mice as a pretreatment, followed by the 648 administration of magnoflorine and induction of colitis using DSS(Fig. 6A). 649 Our results showed no significant differences in body weight, DAI scores, 650 651 colon length, and pathological damage between the ABx-D and ABx-MD groups (Fig. 6B, C and Additional file1: Fig. S4A and B). Furthermore, 652 behavioral tests were conducted to assess the impact of the interventions 653 (Fig. 6D). Notably, no significant differences were observed in the time in 654 center area of OFT and the time in the open arms of EPT between the ABx-D 655 and ABx-MD groups, interestingly, there were significant difference between 656 657 the ABx-C and ABx-D groups. These findings provide valuable insights into the potential influence of the intestinal microbiota on the observed effects of 658 magnoflorine in the context of colitis. 659

To elucidate the potential involvement of the microbiota in the observed effects, we conducted FMT experiments (Fig. 6E). Remarkably, our findings demonstrated that FMT-Mag effectively ameliorated the weight loss, DAI elevation, colon shortening, and histological damage observed in the colitis

mice (Fig. 6F, G and Additional file1: Fig. S4C and D). Moreover, behavioral
assessments revealed notable improvements (Fig. 6H), as evidenced by an
increased the time in the center area of OFT and the time in the open arms
of EPT.

The previous findings indicated that FMT-Mag exhibited potential in 668 669 ameliorating anxiety-like behaviors in colitis mice. However, the underlying mechanism by which the microbiota exerted its effects remained unclear, as 670 671 the bacteria were unlikely to directly cross the blood-brain barrier. Therefore, we hypothesized that the beneficial effects might be mediated by the 672 673 metabolites produced by the microbial colony. To investigate this, we 674 conducted the SFF experiment (Fig. 6I). Remarkably, our results demonstrated that SFF-Mag exhibited the same effects as FMT-Mag, 675 676 SFF-Mag effectively ameliorated the weight loss, DAI elevation, colon shortening, and histological damage observed in the colitis mice (Fig. 6J, K 677 and Additional file1: Fig. S4E and F), and improved colitis-induced anxiety 678 679 behiviours (Fig. 6L). That suggested that the metabolites derived from the magnoflorine-treated microbiota were responsible for the 680 observed 681 improvements in anxiety behavior.

These findings provide valuable insights into the potential mechanisms underlying the beneficial effects of microbiota regulated by magnoflorine and highlight the importance of microbial metabolites in mediating gut-brain axis communication.

686

687 The key bacteria altered by magnoflorine is associated with genes

We conducted RNA-seq analysis on colon tissue samples obtained from 688 Mag+DSS group and DSS group. The results illustrated significant 689 690 differences in the transcriptomes between two groups (Fig. 7A). Subsequently, we conducted a comprehensive analysis of the differentially 691 expressed genes to identify enriched Gene Ontology (GO) terms and Kyoto 692 693 Encyclopedia of Genes and Genomes (KEGG) pathways (Additional file1: Fig. S5A and B). As shown in Fig. 7B, we identified specific KEGG pathways that 694 695 were significantly associated with the differentially expressed genes (P < P)696 0.05), including neuroactive ligand-receptor interaction, PI3K-Akt signaling pathway and MAPK signaling pathway. These results provide valuable 697 698 insights into the molecular mechanisms underlying these biological 699 processes and pathways, which may have implications for next study.

700 Furthermore, we employed the Spearman correlation analysis to examine 701 the associations between the differentially abundant microbiota and the 702 differentially expressed genes (Fig. 7C). Specifically, we observed a positive correlation between Gabrg2 and all the differentially abundant microbiota, 703 704 except for Akkermansia. Conversely, Twist1 displayed a negative correlation 705 with the remaining components of the differentially abundant microbiota. These results shed light on the complex dynamics between host genes and 706 707 the intestinal microbiota, emphasizing the potential significance of these

interactions in shaping host physiology and health.

709

710 Magnoflorine altered the bile acid metabolism in brain

711 Utilizing ADMETlab 2.0²⁷, we computed a LogP value of 0.395 and a BBB Penetration of 0.147 for magnoflorine, suggesting its limited ability to 712 713 traverse the blood-brain barrier. Additionally, a comprehensive literature 714 review revealed consistently low levels of magnoflorine and its metabolites within brain tissue^{28,29}, further corroborating its restricted brain accessibility. 715 Given the previous findings highlighting the potential involvement of the 716 717 intestinal microbiota and its predicted functions, particularly in bile acid 718 metabolism, we hypothesized that magnoflorine may exert its effects on anxiety behavior in colitis mice by modulating bile acid metabolism. To test 719 this hypothesis, we employed targeted metabolomics to assess the levels of 720 bile acids in the brain tissues of colitis mice. Our results revealed the 721 detection of a total of 27 bile acids, we identified a significant increase in 722 723 HDCA and 7-ketolithocholic acid (fold change >2, P < 0.05) in the Mag+DSS group (Fig. 8A). However, HDCA showed the most significant difference in 724 abundance between groups, so we chose HDCA for the follow-up study. 725 These findings provide novel insights into the potential mechanisms 726 underlying the effects of magnoflorine on anxiety behavior in colitis mice, 727 728 highlighting the potential role of bile acid metabolism in mediating gut-brain 729 axis communication.

730

HDCA alleviated anxiety-like behavior and neuroinflammation via TLR4/Myd88 pathway

733 To evaluate the effect of HDCA on colitis-induced anxiety, we induced a mouse model of colitis with 3% DSS orally for 7 days, and observed the 734 735 phenotype of mice after administration of HDCA (500 mg/Kg/d) by gavage (Fig. 8B). HDCA could alleviate colitis (Additional file1: Fig. S6A and B) and 736 737 colitis-induced anxiety (Fig. 8C), as evidence by increasing exploration time in the center area of the OFT, as well as increasing exploration time in open 738 739 arms of EPT. HDCA significantly reduced the expression of mRNA levels of pro-inflammatory factors as shown in Fig. 8D. These suggested that HDCA 740 had a role in alleviating colitis-induced anxiety 741

742 Previous studies and the literature have reported the role of microglia-mediated neuroinflammation involved in the development of 743 anxiety³⁰, we conducted an experiment using BV2 cells. We exposed these 744 745 cells to LPS and simultaneously treated them with HDCA. Our results revealed that LPS administration led to a significant upregulation of TNF- α , 746 IL-1β, and IL-6 mRNA levels and active BV2 cells (Additional file1: Fig. S6C 747 and D). However, the presence of HDCA inhibited this increase in a 748 dose-dependent manner. This suggested that HDCA could alleviate 749 microglia-mediated neuroinflammation. 750

751 To elucidate the underlying mechanism by which HDCA ameliorated

neuroinflammation, 752 microglia mediated we conducted а thorough 753 investigation of relevant genes in microglia using the Genecard database and performed KEGG pathway analysis (Fig. 8E). Our analysis revealed a 754 755 significant enrichment of relevant genes in the Toll-like receptor signaling pathway (P < 0.05). Subsequently, we conducted molecular docking 756 experiments and observed that the ligand-binding domain (LBD) of 757 TLR4/MD2 complex to HDCA was consistent with that to LPS (Fig. 8F). 758 Based on these findings, we hypothesized that HDCA may competitively 759 760 inhibit the binding of LPS to the TLR4/MD2 complex, thereby suppressing 761 the downstream transmission of TLR4 signaling. To validate this hypothesis, 762 as shown in Fig. 8G, we induced an inflammatory response in BV2 cells using LPS and observed a significant increase in the protein levels of Myd88 and 763 764 the downstream effector molecule IL-6. The same phenomenon has been observed in animal experiment (Fig. 8H), indicating HDCA's potential role in 765 alleviating neuroinflammation. So, treatment with HDCA inhibited the 766 767 increase in these proteins, providing further evidence for our hypothesis.

768

769 Discussion

The intricate communication relationship between the gut and the brain, known as the "gut-brain axis", is a crucial factor in the pathogenesis of neurological disorders. Anxiety is a major global challenge, and its prevalence in IBD has reached epidemic proportions, ranging from

5%-20.7%⁶. In this study, we aimed to investigate the specific role of the gut-brain axis in the behavioral mechanism of colitis-induced anxiety. Our findings demonstrated that magnoflorine regulated the intestinal microbiota and increased the HDCA level in brain, alleviated colitis, colitis-induced anxiety behavior and microglia mediated neuroinflammation.

779 Patients with UC are at a high risk of comorbid anxiety, which often predicts a poor prognosis 31,32 . Guidelines recommend screening for 780 781 depression and anxiety for patients with IBD, and drugs for anti-neurological disorders had effective results in IBD patients³³, but these medications often 782 783 come with side effects. Recent study has demonstrated that magnoflorine 784 possesses both anti-inflammatory and moderating effects on neurological disorders³⁴, thus showing potential for development as a dual therapeutic 785 agent for IBD and anxiety-depression. A study investigating the gut 786 microbiota composition of UC patients with and without anxiety and 787 788 depression revealed distinct alterations in microbial diversity and abundance. 789 Notably, patients with UC combined with anxiety and depression exhibited a 790 reduced abundance and diversity of gut flora compared to those without these psychological comorbidities³⁵. Furthermore, specific bacterial taxa 791 792 were found to be associated with depression in IBD patients. Ruminococcus and *Lachnospiraceae* were negatively correlated with depression severity³⁶. 793 These findings suggest a potential link between the depletion of certain 794 795 beneficial gut bacteria and the development of depressive symptoms in IBD

patients and that improving the gut microbiota can alleviate IBD-related anxiety and depression. In our study, magnoflorine administration alleviated colitis-induced anxiety behavior by suppressing microglia mediated neuroinflammation. Our study provides evidence for the potential therapeutic role of magnoflorine in treating colitis-induced anxiety through modulation of the gut microbiota and its metabolites..

The gut barrier is a multifaceted structure comprised of a mucus layer and 802 803 microbiota, an epithelial layer, and a closely interconnected intrinsic layer of 804 immune cells. This barrier acts as a defense mechanism, preventing the 805 entry of harmful substances into the body through the gut, thereby 806 safequarding the body from potential harm. Disruption of its functionality has been linked to IBD³⁷. The integrity of the intestinal barrier function is crucial 807 808 in preventing the entry of pathogen-associated molecular patterns (PAMPs) such as LPS into the body, which can result in the disruption of the 809 blood-brain barrier and ultimately lead to the development of anxiety^{21,38}. 810 811 The negative correlation between barrier function and anxiety development is evident in both the intestinal blood barrier and the blood-brain barrier^{38,39}. 812 813 Our investigation demonstrated that magnoflorine confered protection to the intestinal barrier function. This protection included the up-regulation of tight 814 junction proteins such as ZO-1 and CLDN3, as well as an increase in the 815 expression of goblet cells and MUC2. Furthermore, magnoflorine has been 816 817 shown to enhance the integrity of the blood-brain barrier by upregulating the

818 expression of ZO-1 and PV1.

819 The regulation of gut barrier function is intricately associated with the intestinal microbiota⁴⁰. Certain probiotics, such as *Bifidobacterium*⁴¹ and 820 821 *Ruminococcus*⁴², have the potential to enhance intestinal barrier function. Our investigation has provided evidence for the ability of magnoflorine to 822 823 modulate bacterial microbiota in both healthy and colitis mice. Specifically, we observed an increase in the Verrucomicrobia phylum and a decrease in 824 825 the Firmicutes/Bacteroidetes ratio. Additionally, magnoflorine supplementation led to an increased abundance of beneficial bacteria, 826 827 specially Odoribacteraceae, and a decreased abundance of harmful bacteria. experiments demonstrated 828 Subsequent FMT that FMT from 829 magnoflorine-treated mice effectively protected colitis. This suggests that Odoribacteraceae may play a crucial role in preserving intestinal barrier 830 function. However, there is a notable absence of relevant studies 831 investigating the specific protective mechanisms of Odoribacteraceae in 832 833 colitis.

In addition, we also conducted a comprehensive transcriptome analysis of colitis tissues. Our analysis revealed that differentially expressed genes were significantly enriched in various pathways, including neuroactive ligand-receptor interaction, MAPK signaling pathway, and PI3K Akt signaling pathway. Correlation analysis further unveiled intriguing associations, indicating that *Odoribacteraceae* and *Ruminococcus* exhibited a positive

correlation with Gabrg2, while displayed a negative correlation with Twist1.
Notably, Twist1 is known to regulate immune cell function and upregulated
in patients with corticosteroid-resistant UC^{43,44}. This suggests that *Odoribacteraceae* may confer protection against colitis by inhibiting the
expression of Twist1. However, it is imperative to conduct further
experimental investigations to validate this hypothesis.

Inflammation plays a pivotal role in the pathogenesis of both IBD and 846 neurological disorders. The association between neuroinflammation and 847 anxiety has been extensively documented in numerous studies³⁶. 848 849 Neuroinflammation occurring in various brain regions has been linked to anxiety³⁰. The hippocampus, situated between the thalamus and the medial 850 temporal lobe, is a crucial component of the limbic system involved in 851 cognitive function regulation. It exhibits an intricate neural network of 852 connections with brain regions associated with emotions. Activation of 853 microglia (identified by IBA1 labeling) in the hippocampus leads to the 854 855 production of pro-inflammatory factors such as TNF- α , IL-1 β , and IL-6, consequently promoting anxiety-like behaviors³⁰. LPS serves as a potent 856 stimulant in this regard²¹. Conversely, administration of an oral microglia 857 inhibitor to mice alleviates anxiety-like behavior⁴⁶. Notably, the morphology 858 of microglia reflects their activation status. Our experimental findings 859 revealed heightened microglia activation in the hippocampus and elevated 860 861 levels of the aforementioned pro-inflammatory factors in mice with

862 colitis-induced anxiety. However, the administration of magnoflorine863 effectively inhibits microglia activation.

A study reported that proteins associated with UC combined with anxiety 864 865 and depression clustered in the acute inflammatory response pathway³⁵, In the context of IBD, the intestinal tract serves as a conduit for transmitting 866 inflammatory signals to the brain via three distinct pathways: the 867 systemic-humoral pathway, cellular immune pathway, and neuronal 868 pathway⁴⁷. Disruption of the intestinal barrier function allows the entry of 869 intestinal toxins and inflammatory response factors into the body through the 870 871 gut-blood barrier. Consequently, these inflammatory factors and toxins, 872 including LPS, can breach the blood-brain barrier and gain access to the brain⁴⁸. This breach triggers the activation of immune cells within the brain, 873 874 such as microglia, thereby provoking an inflammatory response that ultimately leads to neurological dysfunction, such as anxiety^{21,48}. Similarly, 875 enterobacterial metabolites can enter the body, some of which exhibit 876 877 protective effects on the blood-brain barrier and can inhibit microglia activation. For instance, SCFAs⁴⁹ and bile acid⁵⁰ fall into this category. Our 878 study utilized SFF experiments to demonstrate the ability of enterobacterial 879 metabolites to mitigate anxiety behaviors induced by colitis. Our findings 880 indicated that the distinct microbiota was linked to bile acid metabolism, as 881 revealed by correlation and differential microbiota analyses. Consequently, 882 883 we proceeded to investigate the levels of bile acids in brain tissues and

observed a significant increase in HDCA levels in the Mag+DSS group.
However, there were still shortcomings in this experiment, as we only
examined the concentration of bile acids in brain tissue, but did not
performed faecal and blood metabolite assays.

HDCA, a natural secondary bile acid, has been shown to alleviate 888 non-alcoholic fatty liver disease by inhibiting intestinal FXR and 889 up-regulating hepatic CYP7B1⁵¹. Intriguingly, both FXR activation and 890 891 inhibition in microglia did not modulate the production of pro-inflammatory mediators⁵².Additionally, HDCA can alleviate sepsis by competitively 892 893 inhibiting the binding of LPS to the TLR4/MD2 complex, and This inhibitory effect was confirmed by surface plasmon resonance (SPR) and cellular 894 experiments⁵³. Furthermore, HDCA has been demonstrated to alleviate 895 896 LPS-induced inflammation by regulating the TGR5/AKT/NF-KB signaling pathway in microglia⁵⁴. Tao Y et al⁵⁵. report that TGR5 knockout mice display 897 anxiety-like behavior. LPS can penetrate the brain by disrupting the 898 899 blood-brain barriers²¹, leading to microglia activation via the TLR4/Myd88 signaling pathway and ultimately resulting in neuroinflammation. Our 900 experiments further confirmed that. 901

902 Conclusions

In conclusion, our investigation demonstrates that the oral administration
of magnolforine modulates the gut-brain axis and mitigates colitis and
colitis-induced anxiety behaviors by influencing intestinal *Odoribacteraceae*

and *Ruminococcus*, as well as the enterobacterial metabolite HDCA.
Furthermore, HDCA competitively inhibits LPS binding to the TLR4/MD2
complex, leading to the inhibition of the TLR4/Myd88 signaling pathway and
subsequent attenuation of neuroinflammation (Fig.9). Our investigation
presents a novel perspective on the therapeutic approach to anxiety
associated with IBD.

912

913 Authors' contributions

HLC and LW conceived and designed the study. LW, MFL, YD, JYW and SQQ
performed the experiments. LYL and SQQ performed the analysis of the data.
LW and MFL wrote the manuscript. BMW, BQL, and HLC revised the
manuscript. All authors read and approved the final manuscript

918 Funding

This work was supported by the National Natural Science Foundation of 919 China under Grant: 82270574, 82070545 and 81970477; the Tianjin Medical 920 921 University General Hospital Fund for Distinguished Young Scholars under 922 Grant: 22ZYYJQ02; the Diversified Fund Project of the Natural Science Foundation of Tianjin, China under Grant: 21JCYBJC00810; the Tianjin Key 923 Medical Discipline (Specialty) Construction Project under 924 Grant: TJYXZDXK-002A. 925

926 Data availability

927 The sequencing data are available on the NCBI site with the project's code

928 PRJNA1067339 and PRJNA1067185.

929 **Declaration of Interest**

- 930 Ethics approval and consent to participate
- 931 The clinical investigation was approved by the ethics committee of the
- 932 Tianjin Medical University, Tianjin, China (Approval NO. IRB2024-YX-152-01).
- All animal experiments were approved by the ethics committee of the Tianjin
- 934 Medical University, Tianjin, China (Approval No. IRB2022-DWFL-074)

935 **Consent for publication**

936 Not applicable.

937 **Competing interests**

938 The authors declare no competing interests.

939 **References**

940 1. Molodecky NA, Soon IS, Rabi DM, Ghali WA, Ferris M, Chernoff G,
941 Benchimol EI, Panaccione R, Ghosh S, Barkema HW, et al. Increasing
942 incidence and prevalence of the inflammatory bowel diseases with time,
943 based on systematic review. Gastroenterology 2012; 142:46-54.e42; quiz
944 e30.

- 945 2. Glassner KL, Abraham BP, Quigley EMM. The microbiome and
 946 inflammatory bowel disease. J Allergy Clin Immunol 2020; 145:16–27.
- 947 3. Liu S, Zhao W, Lan P, Mou X. The microbiome in inflammatory bowel
 948 diseases: from pathogenesis to therapy. Protein Cell 2021; 12:331-45.
- 949 4. Franzosa EA, Sirota-Madi A, Avila-Pacheco J, Fornelos N, Haiser HJ,

Reinker S, Vatanen T, Hall AB, Mallick H, McIver LJ, et al. Gut microbiome
structure and metabolic activity in inflammatory bowel disease. Nat
Microbiol 2019; 4:293–305.

5. Lavelle A, Sokol H. Gut microbiota-derived metabolites as key actors in
inflammatory bowel disease. Nat Rev Gastroenterol Hepatol 2020; 17:22337.

956 6. Bisgaard TH, Allin KH, Keefer L, Ananthakrishnan AN, Jess T. Depression
957 and anxiety in inflammatory bowel disease: epidemiology, mechanisms and
958 treatment. Nat Rev Gastroenterol Hepatol 2022; 19:717-26.

959 7. Barberio B, Zamani M, Black CJ, Savarino EV, Ford AC. Prevalence of
960 symptoms of anxiety and depression in patients with inflammatory bowel
961 disease: a systematic review and meta-analysis. Lancet Gastroenterol
962 Hepatol 2021; 6:359–70.

8. Fairbrass KM, Lovatt J, Barberio B, Yuan Y, Gracie DJ, Ford AC.
Bidirectional brain-gut axis effects influence mood and prognosis in IBD: a
systematic review and meta-analysis. Gut 2022; 71:1773-80.

966 9. Jayasooriya N, Blackwell J, Saxena S, Bottle A, Petersen I, Creese H,
967 Hotopf M, Pollok RCG, POP-IBD study group. Antidepressant medication use
968 in Inflammatory Bowel Disease: a nationally representative population-based
969 study. Aliment Pharmacol Ther 2022; 55:1330-41.

970 10. Mikocka-Walus A, Ford AC, Drossman DA. Antidepressants in
971 inflammatory bowel disease. Nat Rev Gastroenterol Hepatol 2020; 17:184-

972 92.

973 11. Xu T, Kuang T, Du H, Li Q, Feng T, Zhang Y, Fan G. Magnoflorine: A
974 review of its pharmacology, pharmacokinetics and toxicity. Pharmacol Res
975 2020; 152:104632.

976 12. Sakaue S, Kanai M, Tanigawa Y, Karjalainen J, Kurki M, Koshiba S,
977 Narita A, Konuma T, Yamamoto K, Akiyama M, et al. A cross-population atlas
978 of genetic associations for 220 human phenotypes. Nat Genet 2021; 53:1415979 24.

980 13. Peng Y, Yan Y, Wan P, Chen D, Ding Y, Ran L, Mi J, Lu L, Zhang Z, Li X,
981 et al. Gut microbiota modulation and anti-inflammatory properties of
982 anthocyanins from the fruits of Lycium ruthenicum Murray in dextran
983 sodium sulfate-induced colitis in mice. Free Radic Biol Med 2019; 136:96984 108.

985 14. Wu Z, Huang S, Li T, Li N, Han D, Zhang B, Xu ZZ, Zhang S, Pang J,
986 Wang S, et al. Gut microbiota from green tea polyphenol-dosed mice
987 improves intestinal epithelial homeostasis and ameliorates experimental
988 colitis. Microbiome 2021; 9:184.

989 15. Watanabe S, Chen Z, Fujita K, Nishikawa M, Ueda H, Iguchi Y, Une M,
990 Nishida T, Imura J. Hyodeoxycholic Acid (HDCA) Prevents Development of
991 Dextran Sulfate Sodium (DSS)-Induced Colitis in Mice: Possible Role of
992 Synergism between DSS and HDCA in Increasing Fecal Bile Acid Levels. Biol
993 Pharm Bull 2022; 45:1503–9.

994 16. Kihara N. Vanilloid receptor-1 containing primary sensory neurones
995 mediate dextran sulphate sodium induced colitis in rats. Gut 2003; 52:713-9.

996 17. Sobhani Z, Nikoofal-Sahlabadi S, Amiri MS, Ramezani M, Emami SA,

997 Sahebkar A. Therapeutic Effects of Ziziphus jujuba Mill. Fruit in Traditional

and Modern Medicine: A Review. Med Chem 2020; 16:1069-88.

999 18. Li W, Zhang Y, Zhao J, Yang T, Xie J. L-carnitine modified nanoparticles

1000 target the OCTN2 transporter to improve the oral absorption of jujuboside B.

- 1001 Eur J Pharm Biopharm 2024; 196:114185.
- 1002 19. Shi Y-H, Nan Y, Zheng W, Yao L, Liang H-Z, Chen X-J, Song J, Zhang J, Jia
- D-X, Wang Q, et al. [Qualitative and semiquantitative analyses of the
 chemical components of the seed coat and kernel of Ziziphi Spinosae Semen].
 Se Pu Chin J Chromatogr 2024; 42:234–44.
- 1006 20. Bai G, Qiao Y, Lo P-C, Song L, Yang Y, Duan L, Wei S, Li M, Huang S,
- 1007 Zhang B, et al. Anti-depressive effects of Jiao-Tai-Wan on CORT-induced1008 depression in mice by inhibiting inflammation and microglia activation. J
- 1009 Ethnopharmacol 2022; 283:114717.
- 1010 21. Carloni S, Bertocchi A, Mancinelli S, Bellini M, Erreni M, Borreca A,

1011 Braga D, Giugliano S, Mozzarelli AM, Manganaro D, et al. Identification of a

- 1012 choroid plexus vascular barrier closing during intestinal inflammation.
- 1013 Science 2021; 374:439-48.
- 1014 22. Zhao Q, Ren H, Yang N, Xia X, Chen Q, Zhou D, Liu Z, Chen X, Chen Y,
- 1015 Huang W, et al. Bifidobacterium pseudocatenulatum-Mediated Bile Acid

1016 Metabolism to Prevent Rheumatoid Arthritis via the Gut-Joint Axis. Nutrients1017 2023; 15:255.

1018 23. Xu Y, Jing H, Wang J, Zhang S, Chang Q, Li Z, Wu X, Zhang Z. Disordered

1019 Gut Microbiota Correlates With Altered Fecal Bile Acid Metabolism and

1020 Post-cholecystectomy Diarrhea. Front Microbiol 2022; 13:800604.

1021 24. He Z, Ma Y, Yang S, Zhang S, Liu S, Xiao J, Wang Y, Wang W, Yang H, Li

1022 S, et al. Gut microbiota-derived ursodeoxycholic acid from neonatal dairy 1023 calves improves intestinal homeostasis and colitis to attenuate

 $1024 \quad extended \text{-spectrum } \beta \text{-lactamase-producing enteroaggregative Escherichia}$

1025 coli infection. Microbiome 2022; 10:79.

1026 25. Li X, Wang L, Ma S, Lin S, Wang C, Wang H. Combination of Oxalobacter

1027 Formigenes and Veillonella Parvula in Gastrointestinal Microbiota Related to

1028 Bile-Acid Metabolism as a Biomarker for Hypertensive Nephropathy. Int J

1029 Hypertens 2022; 2022:1-14.

1030 26. Sato Y, Atarashi K, Plichta DR, Arai Y, Sasajima S, Kearney SM, Suda W,

Takeshita K, Sasaki T, Okamoto S, et al. Novel bile acid biosynthetic
pathways are enriched in the microbiome of centenarians. Nature 2021;
599:458-64.

1034 27. Xiong G, Wu Z, Yi J, Fu L, Yang Z, Hsieh C, Yin M, Zeng X, Wu C, Lu A, et
1035 al. ADMETlab 2.0: an integrated online platform for accurate and
1036 comprehensive predictions of ADMET properties. Nucleic Acids Res 2021;
1037 49:W5-14.

1038 28. Bao S, Geng P, Wang S, Zhou Y, Hu L, Yang X. Pharmacokinetics in rats
1039 and tissue distribution in mouse of magnoflorine by ultra performance liquid
1040 chromatography-tandem mass spectrometry. Int J Clin Exp Med 2015;
1041 8:20168-77.

- 1042 29. Li B, Han L, Cao B, Yang X, Zhu X, Yang B, Zhao H, Qiao W. Use of
 1043 magnoflorine-phospholipid complex to permeate blood-brain barrier and
 1044 treat depression in the CUMS animal model. Drug Deliv 2019; 26:566–74.
- 1045 30. Guo B, Zhang M, Hao W, Wang Y, Zhang T, Liu C. Neuroinflammation
- 1046 mechanisms of neuromodulation therapies for anxiety and depression. Transl1047 Psychiatry 2023; 13:5.
- 31. Bisgaard TH, Poulsen G, Allin KH, Keefer L, Ananthakrishnan AN, Jess T.
 Longitudinal trajectories of anxiety, depression, and bipolar disorder in
 inflammatory bowel disease: a population-based cohort study.
- 1051 eClinicalMedicine 2023; 59:101986.
- 1052 32. Kim S, Lee S, Han K, Koh S-J, Im JP, Kim JS, Lee HJ. Depression and
- 1053 anxiety are associated with poor outcomes in patients with inflammatory
- 1054 bowel disease: A nationwide population-based cohort study in South Korea.
- 1055 Gen Hosp Psychiatry 2023; 81:68-75.
- 1056 33. Farraye FA, Melmed GY, Lichtenstein GR, Kane SV. ACG Clinical
- 1057 Guideline: Preventive Care in Inflammatory Bowel Disease. Am J
- 1058 Gastroenterol 2017; 112:241-58.
- 1059 34. Okon E, Kukula-Koch W, Jarzab A, Halasa M, Stepulak A, Wawruszak A.

1060 Advances in Chemistry and Bioactivity of Magnoflorine and
1061 Magnoflorine-Containing Extracts. Int J Mol Sci 2020; 21:1330.

35. Yuan X, Chen B, Duan Z, Xia Z, Ding Y, Chen T, Liu H, Wang B, Yang B,
Wang X, et al. Depression and anxiety in patients with active ulcerative
colitis: crosstalk of gut microbiota, metabolomics and proteomics. Gut
Microbes 2021; 13:1987779.

1066 36. Humbel F, Rieder JH, Franc Y, Juillerat P, Scharl M, Misselwitz B,

1067 Schreiner P, Begré S, Rogler G, Von Känel R, et al. Association of Alterations

1068 in Intestinal Microbiota With Impaired Psychological Function in Patients

1069 With Inflammatory Bowel Diseases in Remission. Clin Gastroenterol Hepatol

1070 2020; 18:2019-2029.e11.

1071 37. Kotla NG, Rochev Y. IBD disease-modifying therapies: insights from
1072 emerging therapeutics. Trends Mol Med 2023; 29:241–53.

1073 38. Dion-Albert L, Cadoret A, Doney E, Kaufmann FN, Dudek KA, Daigle B,

1074 Parise LF, Cathomas F, Samba N, Hudson N, et al. Vascular and blood-brain

1075 barrier-related changes underlie stress responses and resilience in female

1076 mice and depression in human tissue. Nat Commun 2022; 13:164.

1077 39. Varanoske AN, McClung HL, Sepowitz JJ, Halagarda CJ, Farina EK,

1078 Berryman CE, Lieberman HR, McClung JP, Pasiakos SM, Philip Karl J. Stress

1079 and the gut-brain axis: Cognitive performance, mood state, and biomarkers

1080 of blood-brain barrier and intestinal permeability following severe physical

and psychological stress. Brain Behav Immun 2022; 101:383-93.

40. Leibovitzh H, Lee S-H, Xue M, Raygoza Garay JA, Hernandez-Rocha C,
Madsen KL, Meddings JB, Guttman DS, Espin-Garcia O, Smith MI, et al.
Altered Gut Microbiome Composition and Function Are Associated With Gut
Barrier Dysfunction in Healthy Relatives of Patients With Crohn's Disease.

1086 Gastroenterology 2022; 163:1364-1376.e10.

1087 41. Song Q, Zhang X, Liu W, Wei H, Liang W, Zhou Y, Ding Y, Ji F, Ho-Kwan

1088 Cheung A, Wong N, et al. Bifidobacterium pseudolongum-generated acetate

1089 suppresses non-alcoholic fatty liver disease-associated hepatocellular

1090 carcinoma. J Hepatol 2023; :S0168827823049814.

- 1091 42. Jia L, Wu J, Lei Y, Kong F, Zhang R, Sun J, Wang L, Li Z, Shi J, Wang Y, et
- 1092 al. Oregano Essential Oils Mediated Intestinal Microbiota and Metabolites
- 1093 and Improved Growth Performance and Intestinal Barrier Function in Sheep.
- 1094 Front Immunol 2022; 13:908015.
- 1095 43. Liu C, Mo L-H, Feng B-S, Jin Q-R, Li Y, Lin J, Shu Q, Liu Z-G, Liu Z, Sun X,

1096 et al. Twist1 contributes to developing and sustaining corticosteroid
1097 resistance in ulcerative colitis. Theranostics 2021; 11:7797-812.

1098 44. Luo Y, Chen J, Liu M, Chen S, Su X, Su J, Zhao C, Han Z, Shi M, Ma X, et

1099 al. Twist1 promotes dendritic cell-mediated antitumor immunity. Exp Cell1100 Res 2020; 392:112003.

1101 45. Van Eeden WA, El Filali E, Van Hemert AM, Carlier IVE, Penninx BWJH,

1102 Lamers F, Schoevers R, Giltay EJ. Basal and LPS-stimulated inflammatory

1103 markers and the course of anxiety symptoms. Brain Behav Immun 2021;

1104 98:378-87.

1105 46. Rooney S, Sah A, Unger MS, Kharitonova M, Sartori SB, Schwarzer C,

1106 Aigner L, Kettenmann H, Wolf SA, Singewald N. Neuroinflammatory

- 1107 alterations in trait anxiety: modulatory effects of minocycline. Transl
- 1108 Psychiatry 2020; 10:256.
- 47. Agirman G, Yu KB, Hsiao EY. Signaling inflammation across the gut-brain
 axis. Science 2021; 374:1087-92.
- 48. Parker A, Fonseca S, Carding SR. Gut microbes and metabolites as
 modulators of blood-brain barrier integrity and brain health. Gut Microbes
 2020; 11:135-57.
- 1114 49. Erny D, Hrabě De Angelis AL, Jaitin D, Wieghofer P, Staszewski O, David
- 1115 E, Keren-Shaul H, Mahlakoiv T, Jakobshagen K, Buch T, et al. Host 1116 microbiota constantly control maturation and function of microglia in the
- 1117 CNS. Nat Neurosci 2015; 18:965–77.
- 1118 50. Bhargava P, Smith MD, Mische L, Harrington E, Fitzgerald KC, Martin K,
- 1119 Kim S, Reyes AA, Gonzalez-Cardona J, Volsko C, et al. Bile acid metabolism is
- altered in multiple sclerosis and supplementation amelioratesneuroinflammation. J Clin Invest 2020; 130:3467-82.
- 1122 51. Kuang J, Wang J, Li Y, Li M, Zhao M, Ge K, Zheng D, Cheung KCP, Liao B,
- 1123 Wang S, et al. Hyodeoxycholic acid alleviates non-alcoholic fatty liver disease
- through modulating the gut-liver axis. Cell Metab 2023; 35:1752-1766.e8.
- 1125 52. Albrecht S, Fleck A-K, Kirchberg I, Hucke S, Liebmann M, Klotz L,

1126 Kuhlmann T. Activation of FXR pathway does not alter glial cell function. J1127 Neuroinflammation 2017; 14:66.

1128 53. Li J, Chen Y, Li R, Zhang X, Chen T, Mei F, Liu R, Chen M, Ge Y, Hu H, et

- 1129 al. Gut microbial metabolite hyodeoxycholic acid targets the TLR4/MD2
- 1130 complex to attenuate inflammation and protect against sepsis. Mol Ther 2023;

1131 31:1017-32.

- 1132 54. Zhu H, Bai Y, Wang G, Su Y, Tao Y, Wang L, Yang L, Wu H, Huang F, Shi
- 1133 H, et al. Hyodeoxycholic acid inhibits lipopolysaccharide-induced microglia
- 1134 inflammatory responses through regulating TGR5/AKT/NF- κ B signaling
- 1135 pathway. J Psychopharmacol (Oxf) 2022; 36:849–59.
- 55. Tao Y, Zhou H, Li Z, Wu H, Wu F, Miao Z, Shi H, Huang F, Wu X. TGR5
 deficiency-induced anxiety and depression-like behaviors: The role of gut
 microbiota dysbiosis. J Affect Disord 2024; 344:219–32.
- 1139

Fig.1 Relationship between anxiety, depression and UC. (A) Proportions of anxiety, depression, sleep disturbance and poor quality of life in UC patients with different disease activity. (B) Linear relationship between GAD-7, PHQ-9 and PSQI, IBDQ. (C) Mendelian randomization: Scatterplot of genetic association between anxiety, depression and UC. Statistical significance was determined using Tukey test. ****P < 0.0001, ns, not significant.

1147 Fig.2 Magnoflorine alleviated DSS-induced colitis. (A) Schematic drug

1148 screening. (B) Experimental scheme of the mouse trial (n = 8). Oral PBS and 1149 magnoflorine treatments were indicated. (C) Daily body weight and daily DAI 1150 scores changes throughout the DSS treatment duration of the study. (**D**) 1151 Images of the colon and the colon length in each group (n = 8). (E) 1152 Concentrations of three representative pro-infammatory cytokines at mRNA level in colon. (F) H&E staining of colon sections and pathological scores of 1153 colons (n = 8). Statistical significance was determined using one-way ANOVA, 1154 followed by Tukey test. **P* < 0.05, ***P* < 0.01, ****P* < 0.001, *****P* < 0.0001. 1155

Fig.3 Magnoflorine protected intestinal barrier function. (A) 1156 1157 Magnoflorine increased ZO-1, CLDN3 expression in colon tissue. Representative Western blot images and densitometric quantification of ZO-1 1158 and CLDN3. Protein levels were normalized to β -actin or GAPDH. (B) 1159 1160 Representative immunofluorescence images and average fluorescence intensity of ZO-1. Magnification: 400 ×, Scale bars: 50µm. (C) 1161 1162 Representative pictures of PAS staining and MUC2 immunohistochemical 1163 staining in colon tissue. Magnification: 400 ×, Scale bars: 50µm. PAS-positive cells and MUC2 production in colonic goblet cells was 1164 significantly enhanced in Mag+DSS group compared to DSS group. 1165 1166 Statistical significance was determined using one-way ANOVA, followed by Tukey test. **P* < 0.05, ***P* < 0.01, ****P* < 0.001, *****P* < 0.0001. 1167

Fig.4 Magnoflorine alleviated colitis-induced anxiety behavior,
 relieved neuroinflammation and protected the blood-brain barrier in

mice. (A) Representative images of mouse trajectories in OFT and EPT 1170 1171 experiments (n = 7). Magnoflorine increased the time and distance in center 1172 area of OFT experiments, increased the time in open arms and decreased the 1173 time in closed arms of EPT experiments. **(B)** Representative 1174immunofluorescence images of ZO-1 and PV-1. Increased expression of ZO1 1175 and PV1 in the choroid plexus of the lateral ventricle in the Mag+DSS group compared with the DSS group. (C) Representative immunohistochemistry 1176 1177 images of Iba-1 in hippocampus CA1 region. Increased endpoints and decreased process length of microglia in the Mag+DSS group compared to 1178 1179 the DSS group (n = 3). (D) Concentrations of three representative pro-infammatory cytokines at mRNA level in hippocampus. Statistical 1180 significance was determined using one-way ANOVA, followed by Tukey test. 1181 1182 *P < 0.05, **P < 0.01, ***P < 0.001, ****P < 0.0001.

Fig.5 Magnoflorine regulated the composition and function of 1183 1184 intestinal microbiota. (A) The relative abundance of fecal bacterial in phyla 1185 level. (B) LEfSe analysis of differences in the microbial taxa between the 1186 Control group and Mag group, and between the DSS group and Mag+DSS group (LDA > 2, P < 0.05). (C) The relative abundance of *Odoribacteraceae* 1187 1188 and Ruminococcus between different groups. (D) WGCNA detected module-traits associations. In the heatmap, each row corresponded to a 1189 module eigengene (ME) and each column to a trait. Each cell contained the 1190 1191 corresponding correlation and p-value. The traits of OFT refers to the time in

1192 central area of OFT. The traits of EPT refers to the times enter in open arms.

Fig.6 Magnoflorine alleviated colitis and anxiety-like behavior 1193 1194 **depending on microbiota.** (A) Study design for the ABx experiment (n = n)1195 5-6). (B) The colon length in each group of ABx. (C) DAI scores change throughout the DSS treatment duration of the ABx experiment. (D) 1196 Representative images of mouse trajectories in OFT and EPT experiments of 1197 the ABx experiment. (E) Study design for the FMT experiment (n = 5-6). (F) 1198 1199 The colon length in each group of FMT. (G) DAI scores change throughout 1200 the DSS treatment duration of the FMT experiment. (H) Representative 1201 images of mouse trajectories in OFT and EPT experiments of the FMT 1202 experiment. FMT-Mag increased the time in center area of OFT experiments, increased the time in open arms of EPT experiments compared to 1203 1204 FMT-Control. (I) Study design for the SFF experiment (n = 5-6). (J) The colon length in each group of SFF. (K) DAI scores change throughout the DSS 1205 treatment duration of the SFF experiment. (L) Representative images of 1206 1207 mouse trajectories in OFT and EPT experiments of the SFF experiment. 1208 SFF-Mag increased the time in center area of OFT experiments, increased 1209 the time in open arms of EPT experiments compared to SFF-Control. Data 1210 were presented as means±SEM. Statistical significance was determined 1211 using one-way ANOVA, followed by Tukey test, or using Tukey test. *P < 0.05, ***P* < 0.01, ****P* < 0.001, *****P* < 0.0001. 1212

1213 Fig.7 Magnoflorine regulated transcriptome expression in colitis

1214 tissues. (A) Volcano plots showed differentially up-regulated and 1215 down-regulated with magnoflorine treatment genes based on 1216 single-dimensional statistical analysis. Red dots indicated the up-regulated 1217 genes and the green dots indicated the down-regulated genes (log2FC > 1, P1218 < 0.05). (B) The KEGG enrichment showed the top 30 representative differential pathways for DEG after magnoflorine treatment (P < 0.05). (C) 1219 The heatmap showed sperman correlation between gut bacteria and hub 1220 genes. Each cell contained the p-value (*P < 0.05, **P < 0.01). 1221

1222 Fig.8 HDCA inhibited neuroinflammation through TLR4/Myd88 1223 pathway. (A) Targeted bile acid metabolism in brain tissue were measured 1224 between the DSS and Mag+DSS mice by LC-MS analysis. (B) Study design for the HDCA experiment (n = 5-6). (C) Representative images of mouse 1225 1226 trajectories in OFT and EPT experiments (n = 5-6). HDCA increased the time 1227 in center area of OFT experiments, increased the time in open arms of EPT 1228 experiments. (**D**) Concentrations of three representative pro-infammatory 1229 cytokines at mRNA level in hippocampus. (E) The top 30 KEGG pathway 1230 based on microglia-related genes of Genecard database. (F) Molecular docking analysis of HDCA on LBD of TLR4/MD2 complex. (G) Western 1231 1232 blotting analysis of TLR4, Myd88 and IL-6 in BV2 cell stimulated by LPS and HDCA. Protein levels were normalized to β -actin. (H) Western blotting 1233 analysis of TLR4, Myd88 and IL-6 in brain hippocampus tissue in HDCA 1234 1235 treatment colitis mice. Protein levels were normalized to β-actin. Statistical 1236 significance was determined using one-way ANOVA, followed by Tukey test.

1237 *P < 0.05, **P < 0.01, ***P < 0.001, ****P < 0.0001.

Fig.9 Schematic summary for the role of magnoflorine in the pathogenesis 1238 1239 of colitis and colitis-induced anxiety. Mice with colitis exhibited gut 1240 microbiota dysbiosis, impaired gut barrier, disrupted blood-brain barrier, 1241 activated microglia, and neuroinflammation, leading to anxiety. Magnoflorine can remodel gut microbiota, increase the abundance of Odoribacteraceae 1242 1243 and Ruminococcus, enhance the concentration of HDCA in the brain. HDCA can alleviate neuroinflammation by inhibiting the TLR4/Myd88 signaling 1244 1245 pathway, thereby alleviating colitis-induced anxiety.

1246

1247 Additional file1

.

Fig. S1 Mendelian randomization Leave-one-out analysis. (A)
Leave-one-out plots for UC on anxiety. (B) Leave-one-out plots for anxiety on
UC. (C) Leave-one-out plots for UC on depression. (D) Leave-one-out plots for
depression on UC.

1252Fig. S2 Magnoflorine affected mice behavior. Magnoflorine increased1253the times enter in open arms of EPT experiments, but not affected immobility1254time in TST and FST experiments. Statistical significance was determined1255using one-way ANOVA, followed by Tukey test. *P < 0.05, ns, not significant.

Fig. S3 Magnoflorine regulated colitis microbiota and WGCNA
analysis. (A) α-diversity upon magnoflorine therapy represented by the

Shannon index, *P < 0.05. (**B**) The PCoA plots upon magnoflorine therapy. (**C**) 1258 1259 STAMP analysis of microbiota at family level between DSS group and 1260 Mag+DSS group. (**D**) By STAMP analysis, 16sRNA sequencing data analyzed 1261 by PICRUSt prediction yielded that K15873 was enriched in the Mag+DSS 1262 K15873: baiH, NAD+-dependent 7beta-hydroxy-3-oxo group. bile acid-CoA-ester 4-dehydrogenase. (E) WGCNA analysis. The left diagram 1263 showed clustering sampletree and cutHeight = 42, the right diagram showed 1264 network topology analysis for different soft-threshold power. The green 1265 1266 arrow indicates the selected power value. (F) Venn diagram showing the 1267 common part of red and blue ME.

Fig. S4 Magnoflorine alleviated colitis depending on microbiota. (A) 1268 Daily body weight change throughout the DSS treatment duration of the ABx 1269 1270 experiment. (B) H&E stained colon sections and Pathological scores of colons of the ABx experiment. (C) Daily body weight change throughout the 1271 1272 DSS treatment duration of the FMT experiment. (D) H&E stained colon 1273 sections and Pathological scores of colons of the FMT experiment.(E) Daily 1274 body weight change throughout the DSS treatment duration of the SFF 1275 experiment. (F) H&E stained colon sections and Pathological scores of colons 1276 of the SFF experiment.. Data were presented as means±SEM. Statistical significance was determined using Tukey test. **P < 0.01, ***P < 0.001, 1277 *****P* < 0.0001. 1278

1279 Fig. S5 GO and KEGG analysis based on DEG between DSS group and

Mag+DSS group. (A) GO functional enrichment analysis, including BP, CC,
and MF. (B) KEGG functional enrichment analysis.

1282 Fig. S6 HDCA alleviated colitis and neuroinfalmmation. (A) Daily body 1283 weight and DAI scores change throughout the DSS treatment duration of the 1284 HDCA treatment experiment. (**B**) Images of the colon and the colon length in HDCA treatment experiment. (C) Concentrations of three representative 1285 pro-infammatory cytokines at mRNA level in BV2 cells. (D) Representative 1286 immunofluorescence images of IBA-1 in BV2 cells. Magnification: 200×, 1287 Scale bars: 50µm. Data were presented as means±SEM. Statistical 1288 significance was determined using Tukey test. *P < 0.05, **P < 0.01, ***P <1289 1290 0.001, ****P < 0.0001.

1291 Additional file2

1292
Table S1 The primer sequences of target genes.
 Table S2 General Clinical
 Features with Remission and Activity in Patients of UC. Table S3 Anxiety, 1293 1294 Depression, Sleep Quality, and Quality of Life in UC Patients in Activity 1295 Compared with in Remission. Table S4 Anxiety, Depression, Sleep Quality, 1296 and Quality of Life in UC Patients in Mild, Moderate, Severe Activity. Table S5 Scores of GAD-7, PHQ-9, PSQI, and IBD-Q in UC Patients in Activity 1297 1298 Compared with in Remission. Table S6 IVs used in MR analysis of the association between UC and anxiety. Table S7 IVs used in MR analysis of 1299 the association between anxiety and UC. Table S8 IVs used in MR analysis 1300 1301 of the association between UC and depression. Table S9 IVs used in MR

1302 analysis of the association between depression and UC.

Figures

Figure 1

() Proportions of anxiety, depression, sleep disturbance and poor quality of life in UC patients with different disease activity. () Linear relationship between GAD-7, PHQ-9 and PSQI, IBDQ. () Mendelian randomization: Scatterplot of genetic association between anxiety, depression and UC. Statistical significance was determined using Tukey test. **** < 0.0001, ns, not significant.

Figure 2

. () Schematic drug screening. () Experimental scheme of the mouse trial (n = 8). Oral PBS and magnoflorine treatments were indicated. () Daily body weight and daily DAI scores changes throughout the DSS treatment duration of the study. () Images of the colon and the colon length in each group (n = 8). () Concentrations of three representative pro-infammatory cytokines at mRNA level in colon. () H&E staining of colon sections and pathological scores of colons (n = 8). Statistical significance was determined using one-way ANOVA, followed by Tukey test. *< 0.05, ** < 0.01, *** < 0.001, **** < 0.0001.

Figure 3

Figure 4

() Magnoflorine increased ZO-1, CLDN3 expression in colon tissue. Representative Western blot images and densitometric quantification of ZO-1 and CLDN3. Protein levels were normalized to β -actin or GAPDH. () Representative immunofluorescence images and average fluorescence intensity of ZO-1. Magnification: 400 ×, Scale bars: 50µm. () Representative pictures of PAS staining and MUC2 immunohistochemical staining in colon tissue. Magnification: 400 ×, Scale bars: 50µm. PAS-positive cells and MUC2 production in colonic goblet cells was significantly enhanced in Mag + DSS group compared to DSS group. Statistical significance was determined using one-way ANOVA, followed by Tukey test. * 0.05, ** 0.01, *** 0.001, **** 0.0001.

Figure 5

() Representative images of mouse trajectories in OFT and EPT experiments (n = 7). Magnoflorine increased the time and distance in center area of OFT experiments, increased the time in open arms and

decreased the time in closed arms of EPT experiments. () Representative immunofluorescence images of ZO-1 and PV-1. Increased expression of ZO1 and PV1 in the choroid plexus of the lateral ventricle in the Mag + DSS group compared with the DSS group. () Representative immunohistochemistry images of Iba-1 in hippocampus CA1 region. Increased endpoints and decreased process length of microglia in the Mag + DSS group compared to the DSS group (n = 3). () Concentrations of three representative pro-infammatory cytokines at mRNA level in hippocampus. Statistical significance was determined using one-way ANOVA, followed by Tukey test. *< 0.05, ** < 0.01, *** < 0.001, **** < 0.0001.

Figure 6

() The relative abundance of fecal bacterial in phyla level. () LEfSe analysis of differences in the microbial taxa between the Control group and Mag group, and between the DSS group and Mag + DSS group (LDA > 2, < 0.05). () The relative abundance of and between different groups. () WGCNA detected module-traits associations. In the heatmap, each row corresponded to a module eigengene (ME) and each column to a trait. Each cell contained the corresponding correlation and p-value. The traits of OFT refers to the time in central area of OFT. The traits of EPT refers to the times enter in open arms.

Figure 7

) Study design for the ABx experiment (n = 5–6). () The colon length in each group of ABx. () DAI scores change throughout the DSS treatment duration of the ABx experiment. () Representative images of mouse trajectories in OFT and EPT experiments of the ABx experiment. () Study design for the FMT experiment (n = 5–6). () The colon length in each group of FMT. () DAI scores change throughout the DSS treatment duration of the FMT experiment. () Representative images of mouse trajectories in OFT and EPT experiment. () Representative images of mouse trajectories in OFT and EPT experiments of the FMT experiment. FMT-Mag increased the time in center area of OFT experiments, increased the time in open arms of EPT experiments compared to FMT-Control. () Study design for the SFF experiment (n = 5–6). () The colon length in each group of SFF. () DAI scores change throughout the DSS treatment duration of the SFF experiment. () Representative images of mouse trajectories in OFT and EPT experiments of the SFF experiment. () Representative images of mouse trajectories in OFT and EPT experiments of the SFF experiment. () Representative images of mouse trajectories in OFT and EPT experiments of the SFF experiment. () Representative images of mouse trajectories in OFT and EPT experiments of the SFF experiment. SFF-Mag increased the time in center area of OFT experiments, increased the time in open arms of EPT experiments compared to SFF-Control. Data were presented as means ± SEM. Statistical significance was determined using one-way ANOVA, followed by Tukey test, or using Tukey test. * < 0.05, ** < 0.01, *** < 0.001, **** < 0.001.

Figure 8

) Volcano plots showed differentially up-regulated and down-regulated genes with magnoflorine treatment based on single-dimensional statistical analysis. Red dots indicated the up-regulated genes and the green dots indicated the down-regulated genes (log2FC > 1, < 0.05). () The KEGG enrichment

showed the top 30 representative differential pathways for DEG after magnoflorine treatment (< 0.05). (C) The heatmap showed sperman correlation between gut bacteria and hub genes. Each cell contained the p-value (* < 0.05, ** < 0.01).

Figure 9

() Targeted bile acid metabolism in brain tissue were measured between the DSS and Mag + DSS mice by LC-MS analysis. () Study design for the HDCA experiment (n = 5–6). () Representative images of mouse trajectories in OFT and EPT experiments (n = 5–6). HDCA increased the time in center area of OFT experiments, increased the time in open arms of EPT experiments. () Concentrations of three representative pro-infammatory cytokines at mRNA level in hippocampus. () The top 30 KEGG pathway based on microglia-related genes of Genecard database. () Molecular docking analysis of HDCA on LBD of TLR4/MD2 complex. () Western blotting analysis of TLR4, Myd88 and IL-6 in BV2 cell stimulated by LPS and HDCA. Protein levels were normalized to β -actin. () Western blotting analysis of TLR4, Myd88 and IL-6 in brain hippocampus tissue in HDCA treatment colitis mice. Protein levels were normalized to β -actin. Statistical significance was determined using one-way ANOVA, followed by Tukey test. * < 0.05, ** < 0.01, *** < 0.001, **** < 0.001.

Figure 10

Schematic summary for the role of magnoflorine in the pathogenesis of colitis and colitis-induced anxiety. Mice with colitis exhibited gut microbiota dysbiosis, impaired gut barrier, disrupted blood-brain barrier, activated microglia, and neuroinflammation, leading to anxiety. Magnoflorine can remodel gut microbiota, increase the abundance of and , enhance the concentration of HDCA in the brain. HDCA can alleviate neuroinflammation by inhibiting the TLR4/Myd88 signaling pathway, thereby alleviating colitis-induced anxiety.

Figure 11

Figure 12

Figure 13

Figure 14

Figure 15

Figure 16

Figure 17

Figure 18

Supplementary Files

This is a list of supplementary files associated with this preprint. Click to download.

- Additionalfile1.docx
- additionalfile2tableS1.xls
- additionalfile2tableS2.xls
- additionalfile2tableS3.xls
- additionalfile2tableS4.xls
- additionalfile2tableS5.xls
- additionalfile2tableS6.xls
- additionalfile2tableS7.xls
- additionalfile2tableS8.xls
- additionalfile2tableS9.xls
- Additionalfile1.docx
- additionalfile2tableS1.xls
- additionalfile2tableS2.xls
- additionalfile2tableS3.xls
- additionalfile2tableS4.xls
- additionalfile2tableS5.xls
- additionalfile2tableS6.xls
- additionalfile2tableS7.xls
- additionalfile2tableS8.xls

• additionalfile2tableS9.xls